

A Lagrangian Dynamical Theory for the Mass Function of Cosmic Structures: I Dynamics

Pierluigi Monaco

Scuola Internazionale Superiore di Studi Avanzati (SISSA), via Beirut 4, 34014 – Trieste, Italy

Dipartimento di Astronomia, Università degli studi di Trieste, via Tiepolo 11, 34131 – Trieste, Italy

Email: monaco@sissa.it

ABSTRACT

A new theory for determining the mass function of cosmic structures is presented. It relies on a realistic treatment of collapse dynamics. Gravitational collapse is analyzed in the Lagrangian perturbative framework. Lagrangian perturbations provide an approximation of truncated type, i.e. small-scale structure is filtered out. The collapse time is suitably defined as the instant at which orbit crossing takes place. The convergence of the Lagrangian series in predicting the collapse time of a homogeneous ellipsoid is demonstrated; it is also shown that third-order calculations are necessary in predicting collapse. Then, the Lagrangian prediction, with a correction for quasi-spherical perturbations, can be used to determine the collapse time of a homogeneous ellipsoid in a fast and precise way. Furthermore, ellipsoidal collapse can be considered as a particular truncation of the Lagrangian series. Gaussian fields with scale-free power spectra are then considered. The Lagrangian series for the collapse time is found to converge when the collapse time is not large. In this case, ellipsoidal collapse gives a fast and accurate approximation of the collapse time; spherical collapse is found to poorly reproduce the collapse time, even in a statistical sense. Analytical fits of the distribution functions of the inverse collapse times, as predicted by the ellipsoid model and by third-order Lagrangian theory, are given. These will be necessary for a determination of the mass function, which will be given in paper II.

Key words: cosmology: theory – dark matter – large-scale structure of the Universe

1 INTRODUCTION

An important outcome of any cosmological model is the distribution of the masses of those collapsed clumps which form during gravitational collapse; this quantity is usually called mass function (hereafter MF), or multiplicity function. These structures correspond to the observed galaxies, groups and clusters of galaxies. Thanks to recent efforts, the masses of these observed cosmic structures can be estimated, though with large uncertainties and relying on uncertain hypothesis. Galaxy cluster masses can be estimated by means of three different methods: estimates based on optical galaxies, such as virial estimates (Biviano et al. 1993; see also Bahcall & Cen 1993), X-ray temperatures (Henry & Arnaud 1991), and gravitational lensing (see, e.g., Fort & Mellier 1994). Every method has its drawbacks: virial estimates rely on the delicate hypothesis of virial equilibrium; X-ray analyses rely on safer gas-dynamical hypotheses but are confined to the inner regions of the cluster; lensing estimates directly probe the gravitational potential, but are now available only for a few clusters. Group masses are much more difficult to estimate, due to the small number

of galaxies involved and to the uncertain dynamical status of groups. Virial mass estimates, corrected for unvirialization, are available for a large number of groups (Pisani et al. 1992). Galaxy masses are relatively easier to determine, due to the more evolved dynamical status and to the large number of tracers (stars instead of galaxies) (see Ashman, Persic & Salucci 1993). However, mass estimates are mainly limited to a few optical radii, while dark-matter halos probably extend further.

The state of the art of the MF theory presents severe problems as well. Cosmological structures are the sites of highly non-linear dynamics; it is well known that, for generic initial conditions, the Newtonian collapse of a general self-gravitating system has no known solution in the highly non-linear regime. Analytical approximations and N-body simulations can help to face the problem in an approximate way. In this paper I will mainly focus on realistic analytical approximations to gravitational collapse, needed to develop a MF theory. Another paper (Monaco 1996, hereafter paper II) develops the statistical tools necessary to get a MF.

Despite the intrinsic difficulties, a heuristic solution of the MF problem was found as early as 1974 by Press &

Schechter (1974; hereafter PS). I have already described in full detail the PS MF in a previous paper (Monaco 1995; hereafter M95). It suffices now to recall that all the dynamical difficulties of non-linear dynamics are circumvented by assuming that ‘something happens’ to a mass clump (i.e. a fully virialized structure forms) as soon as its linearly evolved density contrast δ reaches a given threshold δ_c of order one. One of the simplest fully non-linear collapse models, the spherical model, can be invoked to give a more precise determination of the quantity δ_c : indeed, the spherical model predicts full collapse to a singularity as soon as the linearly extrapolated density contrast reaches $\delta_c=1.69$. Surprisingly, the PS formula has been found to reproduce in a more or less accurate way the results of large N-body simulations (see references and discussions in M95). Comparisons of the PS MF to N-body simulations have often suggested a lower value for the δ_c parameter, even though technical details, such as the group-finding algorithm and the shape of the filter function, have to be taken into account to obtain a precise number. The original PS formulation has been improved in a number of papers; in particular, Peacock & Heavens (1990) and Bond et al. (1991) have solved the so-called ‘cloud-in-cloud’ problem, while Bower (1991) and Lacey & Cole (1993, 1994) have extended the formalism to describing merging histories of dark matter halos. A more complete list of references and a deep discussion on these points is given in paper II.

It is worth stressing that the only dynamical ingredients of the PS recipe are linear theory and a fixed density threshold. Thus, the PS MF can only be considered as a fitting formula which nicely describes the results of many N-body simulations. A great advantage in using only linear theory is the following: as linear theory predicts the density field to be rescaled, as it evolves, by a factor which depends only on time, the statistical properties of the final field are the same as the initial field, which is usually assumed to be a Gaussian process. In practice, evolved density fields develop strong and non-trivial non-Gaussian features. Nonetheless, most works on the MF, since that of PS, have detailed the statistical treatment of regions with initial density larger than a given threshold (called ‘excursion sets’), or peaks of the initial density field, rarely detailing the dynamical description of collapse.

Only a few authors have considered more evolved dynamics than linear theory. Lucchin & Matarrese (1988) and Porciani et al. (1996), in two different ways, introduced non-Gaussianity into the MF. In Lucchin & Matarrese (1988) the non-Gaussianity was explicitly introduced in a PS-like approach; it could be either primordial or of dynamical origin. Porciani et al. (1996) introduced non-Gaussianity in the framework of diffusion theory (Bond et al. 1991), by putting a reflecting barrier at $\delta = -1$, to avoid unphysical negative densities. In both cases, gravitationally-induced non-Gaussianity was found to cause enhanced production of high-mass clumps, and, in Porciani et al. (1996), an intriguing cut-off at low masses was predicted. Vergassola et al. (1994) calculated the MF in the framework of adhesion theory; collapsed structures were identified with caustics. Another attempt to model in a more realistic way the formation of collapsed clumps was made by Bond & Myers (1996), in the framework of peak-patch theory. In that theory, the collapse times of the peak-patches were estimated by means of the homogeneous ellipsoidal collapse model, and the final

locations were found by means of Zel’dovich (1970) approximation. Ellipsoidal collapse in a cosmological context was used also by Eisenstein & Loeb (1995) to estimate the angular momentum of collapsing structures.

A very different approach was used by Cavaliere and collaborators in a number of works (see Cavaliere, Menci & Tozzi 1994 for a recent review). First they constructed a MF theory based on dynamical timescales, then they used a kinetic approach to model the aggregation of already collapsed clumps, and finally they found a formalism, based on Cayley trees, which was able to unify the kinetic and diffusion approaches. They recently applied this formalism to adhesion theory (Cavaliere, Menci & Tozzi 1996). Similar or related approaches were recently used by Shaviv & Shaviv (1995) and by Sheth (1996). Such approaches, very different from the ones mentioned above, attempt to describe the highly non-linear behaviour of matter clumps after first collapse.

In a previous paper, M95, I attempted to introduce realistic dynamics in the framework of a PS-like theory. The PS idea of identifying the fraction of collapsed matter as the probability that a point fulfills certain collapse conditions was used to determine the MF. It was shown that such kind of approach greatly simplifies if ‘local’ predictions of collapse are used, i.e. if the collapse of a mass element is based on some relevant quantities *relative only to the element considered*. Collapse predictions were estimated by means of an ansatz based on the Zel’dovich approximation and by means of the homogeneous ellipsoid collapse model. The result was an increase in large-mass objects with respect to the usual PS prediction, which could explain why lower δ_c values than the spherical 1.69 are found when comparing the PS MF to N-body simulations (lower values of δ_c correspond to a shift of the large-mass tail of the MF toward large masses).

The M95 work can be seen as a simple ‘variation on a theme’ of the PS procedure, plagued by all the PS faults, e.g. the cloud-in-cloud problem. Anyway, that variation suffices in shedding light on a number of problems which have a precise dynamical meaning, and which are connected to the use of the spherical collapse model. To be more precise, the spherical model predicts full collapse of the whole structure to a singularity at a given time; it is usually assumed that at that time the structure fully virializes. In this way: (i) collapse is quite well defined and (ii) virialization surely occurs (iii) at the same moment as the collapse, so that the two concepts can be used equivalently. In practice, when collapse takes place with a realistic geometry, (i) it has to be carefully defined, and different authors have in fact different ideas on what collapse is (e.g., is the ‘real’ collapse of a homogeneous ellipsoid that on the first axis, or that on all three axes?); (ii) while it is somehow possible to model collapse, it is terribly difficult to model virialization, and it is terribly difficult to decide when and where virialization is going to have place (clusters and groups of galaxies are generally *not* virialized!).

In this paper, and in paper II, the ideas contained in M95 are pushed further, in order to construct a complete theory of the mass distributions of cosmic structures, based on realistic dynamics. This paper focuses on the dynamical estimate of the collapse time of a mass element, and on the definition of collapse. Paper II will be concerned with the statistics necessary to get a MF from the definition of

collapse and its distribution. The whole set-up of the dynamical problem is based on the idea, already formulated in M95, that the MF is an intrinsically Lagrangian quantity, in the sense that it is best faced within the framework of Lagrangian fluidodynamics. In Section 2 the machinery of Lagrangian dynamics of a cosmological self-gravitating cold fluid is presented. Lagrangian perturbation theory is introduced: it provides an excellent framework to estimate the collapse time of a mass element. In Section 3 the definition of collapse is analyzed, its punctual, non-local nature is stressed, and a way of defining collapse in the case of non-filtered fields is presented; this can be implemented as the collapse definition when comparing this theory to N-body simulations. In Section 4 the Lagrangian perturbative series, up to the 3rd order, is successfully applied to the homogeneous ellipsoid collapse. In Section 5 the collapse of a Gaussian field with power-law spectra, generated in cubic grids of 32^3 points, is carefully analyzed. As a result, the simple ellipsoidal model is found to give a very accurate estimate of the collapse time, at least for the largest objects which collapse. The distribution of the inverses of collapse times is analyzed and quantified; this quantity is necessary for the calculation of the MF. Section 6 contains a summary and conclusions. Technical details about Lagrangian perturbations and ellipsoidal collapse are given in two Appendices.

2 THE LAGRANGIAN NATURE OF THE MASS FUNCTION

The MF is the distribution of the masses of the collapsed, isolated clumps of mass. To get a MF, information about the mass elements which undergo collapse is needed; it is not necessary to know where the collapsed clumps go to. Then, the MF problem is suitably analyzed in a Lagrangian fluidodynamical framework, where the independent space variable \mathbf{q} is related to a given mass element, whose motion is followed. This is different from the usual Eulerian picture, where the space variable \mathbf{x} is related to a given spatial point, and the evolution of the elements, which instantaneously happen to be in that point, is followed. This is the starting point of the MF theory presented here. Recently, the same point of view has been taken by Audit & Alimi (1996).

Consider a pressureless, unvortical, Newtonian, self-gravitating fluid in a perturbed Friedmann-Robertson-Walker Universe, with given cosmological parameters Ω_0 and Λ . The trajectory \mathbf{x} of every (infinitely small) mass element, initially at the comoving position \mathbf{q} , can be written as:

$$\mathbf{x}(\mathbf{q}, t) = \mathbf{q} + \mathbf{S}(\mathbf{q}, t). \quad (1)$$

\mathbf{S} is the displacement field (in comoving coordinates). All the kinematic quantities relative to the mass element and its density contrast can be expressed in terms of the displacement \mathbf{S} (see Appendix A, equation A1). Note that, in this approach, the density is not a dynamical quantity, as it was in the Eulerian approach; the only dynamical quantity here is the displacement field \mathbf{S} . It is possible to find evolution equations for \mathbf{S} , equivalent to the usual Euler-Poisson system for the Newtonian evolution of perturbations. Several authors, namely Buchert (1989), Bouchet et al. (1995),

Lachièze-Rey (1993b) and Catelan (1995), have written different equivalent forms of the same system of equations for \mathbf{S} . The equations of Catelan (1995) are reported in Appendix A. In the following it will always be assumed that the initial velocity field is irrotational and parallel to the gravitational acceleration; see Appendix A for further details.

It is possible to give initial conditions for the system through the initial peculiar rescaled gravitational potential $\varphi(\mathbf{q}, t_0)$, instead of the usual initial density contrast $\delta(\mathbf{q}, t_0)$; the two fields are simply related by a Poisson equation:

$$\nabla^2 \varphi(\mathbf{q}, t_0) = \frac{\delta(\mathbf{q}, t_0)}{b(t_0)}, \quad (2)$$

where $b(t)$ is the linear growing mode (note that $b(t_0) \simeq a(t_0)$).

An important quantity is the Jacobian determinant of the transformation given in equation (1):

$$J(\mathbf{q}, t) = \det \left(\frac{\partial x_a}{\partial q_b} \right) = \det(\delta_{ab} + S_{a,b}) \quad (3)$$

(comma denotes \mathbf{q} -derivative); the quantity $S_{a,b}$ is commonly called *deformation tensor*. The Lagrangian approach has a natural limit in the condition $J = 0$. Before this moment, the Lagrangian-to-Eulerian mapping is single-valued (single-stream or laminar regime), i.e. mass elements coming from different points of (Lagrangian) space do not arrive at the same Eulerian position. When $J = 0$ (orbit crossing or shell crossing, hereafter OC) the $\mathbf{q} \rightarrow \mathbf{x}$ mapping becomes multi-valued (multi-stream regime), and the density, being proportional to the inverse of J , goes to infinity (see Shandarin & Zel'dovich 1989 for a discussion of caustic formation). It is beyond the scope of this paper to discuss the possibility of using a Lagrangian approach in the multi-stream regime; see Buchert (1994) for a discussion. Here it has to be noted that OC takes place as soon as the first objects collapse, which, for any realistic power spectrum, happens very soon after recombination. So the Lagrangian formulation is, as it stands, essentially useless unless the initial (potential or density) field is smoothed to truncate the small-scale part of the power spectrum. This is a key point: from a field $\varphi(\mathbf{q})$, which can in principle have power on all scales, a hierarchy of smooth fields is worked out:

$$\varphi(\mathbf{q}) \rightarrow \varphi(\mathbf{q}; R_f), \quad (4)$$

where R_f is the width of the filter (the two fields are both freely called φ , but they are in fact different mathematical objects). This highlights the strongest hypothesis of this theory, namely that small-scale structure does not influence in a significant way the dynamical evolution of larger scales before OC. All the following considerations apply to a general element of the $\varphi(\mathbf{q}; R_f)$ hierarchy, i.e. to a smoothed version of φ ; the parameter R_f will be omitted for simplicity's sake. (Note that some approximation schemes, such as adhesion theory (Gurbatov, Saichev & Shandarin 1989) or frozen flow approximation (Matarrese et al. 1992), avoid OC; in this case no smoothing of the initial field is needed in principle.)

The Lagrangian evolution equations for \mathbf{S} , as well as the Eulerian evolution equations for δ , have not been solved in general cases. Nonetheless, it is possible to find, as in the Eulerian case, perturbative solutions. In the Eulerian case (see, e.g., Bouchet 1996), the equations are expanded

in terms proportional to powers of the density contrast; if this quantity is small, then successive perturbative terms are increasingly smaller and the series converges. As a consequence, the validity of the Eulerian perturbative scheme is limited to small density contrasts. In the Lagrangian case, the perturbed quantity is not the density, which is not a dynamical quantity, but the (comoving) displacements of the particles from their initial positions. It is easy to understand why this simple change of perturbing parameter causes dramatic improvements in the performances of the approximations: the density, being proportional to the inverse of J (equation A1), becomes infinite when J goes to 0. In this case, at least some matrix element of the deformation tensor (e.g. one eigenvalue, if $S_{a,b}$ is symmetric) is of order (minus) one, i.e. just at the limit of validity of the perturbation scheme. In other words, when Lagrangian perturbations start to break down, the density can have reached very large values.

A number of authors have analyzed the Lagrangian perturbation scheme at various orders, up to the third (Buchert 1989; Moutarde et al. 1991; Bouchet et al. 1992; Buchert 1992; Buchert & Ehlers 1993; Lachièze-Rey 1993a,b; Bouchet et al. 1995; Buchert 1994; Catelan 1995; Bouchet 1996; Buchert 1996). A brief list of the main results is given in Appendix A; see the references for further details. As a matter of fact, different authors use very different notations; the notation I will use is similar to that of Catelan (1995).

The perturbative series for \mathbf{S} can be written, up to third order, as:

$$\mathbf{S}(\mathbf{q}, t) = b_1(t)\mathbf{S}^{(1)}(\mathbf{q}) + b_2(t)\mathbf{S}^{(2)}(\mathbf{q}) + b_{3a}(t)\mathbf{S}^{(3a)}(\mathbf{q}) + b_{3b}(t)\mathbf{S}^{(3b)}(\mathbf{q}) + b_{3c}(t)\mathbf{S}^{(3c)}(\mathbf{q}) + \dots \quad (5)$$

In the following, among models with $\Lambda \neq 0$, only the flat ones will be considered (the others are not of great cosmological interest). The time functions $b_n(t)$ are given in Appendix A, equations (A7). The first-order time function is just (minus) the linear growing mode, $b_1(t) = -b(t)$, while the others are, at leading order and with great accuracy (exactly for an Einstein-de Sitter background), proportional to b^2 or b^3 , according to their order. This means that, in all the calculations that follow, the dependence on the background cosmology can be factorized out by using $b(t)$ as time variable. The spatial equations for the $\mathbf{S}^{(n)}(\mathbf{q})$ terms are Poisson equations; this reflects the implicit non-locality of Newtonian gravitational dynamics. Again, they are reported in Appendix A. Note that the $\mathbf{S}^{(2)}$, $\mathbf{S}^{(3a)}$ and $\mathbf{S}^{(3b)}$ terms are irrotational ($S_{a,b}^{(n)}$ is symmetric), while the $\mathbf{S}^{(3c)}$ term is purely rotational ($S_{a,b}^{(3c)}$ is antisymmetric).

It is easy to recognize that the linear term of the perturbation,

$$\mathbf{x} = \mathbf{q} - b(t)\nabla\varphi, \quad (6)$$

is the well-known Zel'dovich (1970) approximation. This is not the place to list all the features, merits and limits of this approximation; the reviews of Shandarin & Zel'dovich (1989) and Sahni & Coles (1995) give full details and complete reference lists. Some comments were reported also in M95. It is worth mentioning that Zel'dovich and 2nd order truncated approximations have been found very successful in predicting the evolution of a N-body matter field in

the weakly non-linear regime, according to cross-correlation tests (Coles, Melott & Shandarin 1993; Melott, Buchert & Weiß 1995; Sahni & Coles 1995). The third order has not been found to increase significantly the precision of the series; moreover, third-order terms are very sensitive to numerical errors, so the use of third-order predictions is not generally recommended in that context. Another general conclusion is that the 3c term does not have great influence on the density evolution (see also Buchert et al. 1997), which is to be expected, as this term, being purely rotational, corresponds to a rotation of the mass element in Lagrangian space, which does not influence the density by itself.

As already noted in M95, there is a key difference between the usual applications of the truncated Lagrangian approximations and the one which is to be used here. In the works cited above the density fields are evolved up to mass variances of order 1 or slightly more; at this level the convergence of the Lagrangian series is more or less guaranteed by construction. But the MF needs a prediction of collapse, when all the perturbative terms become of the same order. The convergence of the series in this case is not guaranteed and has to be checked. This will be done in Section 4 in the case of ellipsoidal collapse, and in Section 5 in the case of Gaussian fields with scale-free power spectra.

3 THE DEFINITION OF COLLAPSE

The key quantity for the determination of a MF is the instant at which a given mass element collapses. This raises the not trivial question of what collapse means. Within the Lagrangian perturbation framework, there is a natural definition of collapse:

$$J(\mathbf{q}, b_c) = 0 \quad (7)$$

(note that the linear growing mode b is the time variable; b_c is the collapse time). This instant has already been defined before as OC. At this instant a number of things happen: (i) the density becomes infinite; (ii) the other kinematic quantities become infinite (see M95); (iii) different trajectories intersect; (iv) multi-stream regions form; (v) shock waves can form in a (subdominant) dissipative component (baryons); (vi) gravitational dynamics becomes interesting and (vii) really difficult to follow. After OC a number of other things can happen: violent relaxation, virialization, gas cooling, star formation, supernovae feedback etc. All these relevant events are decisive in making real astrophysical structures, but are very difficult to model. Surely OC is a necessary condition for these events to take place.

The main interest of the present theory is to model dark matter clumps, not astrophysical objects. Dark matter clumps can be thought of as local high-density concentrations of matter, regardless of their geometry, internal dynamical status (relaxation, virialization or otherwise) and so on. Then the above definition of collapse is meaningful, provided a mass element which has undergone collapse remains in some high density clump; I assume that this is the case. This assumption is reasonable: were it not the case, mass elements entering a structure would evaporate back into the background soon after; such evaporation events are assumed to be rare.

It is opportune not to introduce conditions on the internal dynamical status of a collapsed clump at the level of collapse definition, for at least two good reasons: (i) dynamics in the multi-stream regime is not well understood, and any oversimplification, such as virialization soon after collapse, can be misleading. (ii) Real objects, as groups and clusters of galaxies, have plausibly undergone some kind of (violent) relaxation, but their state is very complicated; only the cores of rich groups and clusters are observed in a more evolved state. Furthermore, a collapsed but not dynamically evolved clump may contain smaller, more relaxed or fully virialized clumps, which can survive in the larger structure for a significant time; this could be the situation of galaxies in groups. This kind of MF theory cannot provide a description of such subclumps, or, in other words, cannot represent galaxies in groups or clusters. A kinetic approach like that described in Cavaliere et al. (1994) can model this kind of objects.

Another key feature of this definition is that it is clearly *punctual*, in the sense that any prediction is relative to a point. It is often assumed in the literature that the collapse prediction of a point is to be extended to a surrounding region of filter-width size, as the prediction is based on a mean over a given region; this fact, reasonable especially when top-hat smoothing is used, leads to some complications in the MF, as Blanchard, Valls-Gabaud & Mamon (1992) and Yano, Nagashima & Gouda (1996) have shown. This is not my point of view: filtering of the initial field is only necessary to suppress small-scale orbit-crossed regions. All the kinematic and dynamical quantities, and then the collapse predictions, are strictly punctual, defined on vanishingly small mass elements. On the other hand, if the field is smooth on a scale R_f , the collapse predictions will show a coherence on a scale R_f , without any further assumptions.

Summing up, the definition of collapse given by equation (7) can reasonably reproduce high-density clumps, regardless of their internal dynamical status. Due to the truncated nature of the approximations used, collapsed regions are predicted to reach infinite density, but actual collapsing regions contain smaller-scale structures which spread the collapsing mass around, thus lowering the true density. It is worthwhile wondering how a clump, which is predicted to collapse when the field is smoothed at a given scale, can be recognized in the unsmoothed evolved system, e.g., in a N-body simulation. Any conventional clump-finding algorithm, based on percolation or overdensities above a given threshold, will probably find more easily those collapsed regions which have certain geometries, e.g. spherical rather than filamentary. The choice of the clump-finding algorithm is decisive in this case, and it is opportune to choose an algorithm based on the collapse definition given above, equation (7). A good choice is to construct an algorithm based simply on the concept of mapping, as infinite density is only a consequence. I propose the following formula as an implementation of equation (7):

$$\exists \mathbf{q}_1, \mathbf{q}_2 : |\mathbf{q}_1 - \mathbf{q}_2| \geq L, \quad (8)$$

$$|\mathbf{x}(\mathbf{q}_1, b) - \mathbf{x}(\mathbf{q}_2, b)| < \varepsilon, \quad \varepsilon \ll L,$$

where both \mathbf{q}_1 and \mathbf{q}_2 are collapsed, relative to a scale L , at the time $b > b_c$. This definition is very easy to implement in an N-body simulation.

Obviously, a tight correspondence between high-density clumps and regions found with equation (8) is expected, especially for the most massive clumps. Nonetheless, the precise relationship has to be checked with N-body simulations. In any case, the ‘objects’ predicted by this kind of theory are interesting in themselves, as they are the sites of highly non-linear dynamics, and surely contain the mass which is going to form astrophysical and cosmological objects. If more restricted classes of objects are needed, the possibility of getting them by placing further constraints on the collapsing point would be worth exploring. As a conclusion, to be conservative the MF which can be found with such a definition of collapse could be called the MF of *high non-linearity environments*.

4 LAGRANGIAN PERTURBATIONS IN HOMOGENEOUS ELLIPSOIDAL COLLAPSE

As a first step, the gravitational collapse of a homogeneous triaxial ellipsoid is considered. This exercise is useful for testing the convergence of the Lagrangian series at OC, which is not guaranteed by construction. Consider the potential:

$$\varphi(\mathbf{q}) = \frac{1}{2}(\lambda_1 q_1^2 + \lambda_2 q_2^2 + \lambda_3 q_3^2), \quad (9)$$

where the λ_i are the eigenvalues of the first-order deformation tensor $S_{a,b}^{(1)} = \varphi_{,ab}$; note the difference of sign from the definition in M95. They are ordered as follows: $\lambda_1 \geq \lambda_2 \geq \lambda_3$. Because of Poisson equation (2), $\delta_i \equiv \delta(t_0)/b_0 = \lambda_1 + \lambda_2 + \lambda_3 = \text{const}$. Equation (9) represents the potential of a homogeneous ellipsoid in its principal reference frame.

With this potential it is possible to solve all the Poisson equations for the perturbing potentials. All the details of the calculations are contained Appendix B. The solutions can be directly found by using the so-called ‘local forms’ of the perturbing potentials, which can be found in Buchert & Ehlers (1993), Buchert (1994) and Catelan (1995). Briefly, it is possible to find vector fields, functions of the initial potential and its derivatives *in the point considered*, which solve the spatial equations (A13), but are generally not irrotational. The local form $\mathbf{S}^{(2L)}$ of the second-order displacement is:

$$\mathbf{S}^{(2)} = [\nabla\varphi(\nabla^2\varphi) - (\nabla\varphi \cdot \nabla)\nabla\varphi] + \mathbf{R}^{(2)} = \mathbf{S}^{(2L)} + \mathbf{R}^{(2)}. \quad (10)$$

The vector $\mathbf{R}^{(2)}$, divergenceless, is added to the local form $\mathbf{S}^{(2L)}$ in order to keep the vector $\mathbf{S}^{(2)}$ irrotational; it contains the deep non-locality of gravitational dynamics. Analogous expressions for the 3a, 3b and 3c contributions are reported in Appendix B. The local forms are solutions of equations (A13) if they are irrotational by themselves; this happens only for a restricted class of initial conditions, to which the homogeneous ellipsoidal potential belongs. Then the local forms can be used to promptly obtain the perturbing potentials of the ellipsoid.

The 2nd-order local contribution to the deformation tensor, $S_{a,b}^{(2L)}$, contains terms with second derivatives of φ and mixed terms with first and third derivatives. In the homogeneous ellipsoidal case only the second derivative terms survive. The same happens for the 3aL and 3bL terms, while the 3cL term is null (see Appendix B). I call *ellipsoidal parts* those terms of the local contributions to the deformation tensor which survive in the ellipsoidal case:

$$\begin{aligned}
S_{a,b}^{(2E)} &= \varphi_{,ab}\varphi_{,cc} - \varphi_{,ac}\varphi_{,bc} \\
S_{a,b}^{(3aE)} &= \varphi_{,ac}\varphi_{,bc}^C \\
S_{a,b}^{(3bE)} &= \frac{1}{2}[S_{ab}^{(2E)}\varphi_{,cc} - S_{bc}^{(2E)}\varphi_{,ac} + \varphi_{,ab}S_{c,c}^{(2E)} - \varphi_{,bc}S_{a,c}^{(2E)}] \\
S_{a,b}^{(3cE)} &= 0;
\end{aligned} \tag{11}$$

$\varphi_{,ab}^C$ is the cofactor matrix of $\varphi_{,ab}$. These terms can be considered as a truncation of the local form, when all derivatives of φ greater than the second are neglected. (Note that 2nd-order local and ellipsoidal displacements, \mathbf{S}^{2L} and \mathbf{S}^{2E} , are equal, as the local form contains up to second derivatives of the initial potential; the differences appear in the deformation tensor. Third-order local and ellipsoidal displacements are instead different.)

If the very weak Ω dependence of the time functions is neglected (see equations A7), the collapse equation $J = 0$ is simply an algebraic equation in the variable $b(t)$ (the growing mode), of order equal to the Lagrangian order. All the technical details are reported in Appendix B. In the spherical case, in which $\lambda_1 = \lambda_2 = \lambda_3 = \delta_l/3$, the collapse times predicted by the Lagrangian series up to the 1st-, 2nd- and 3rd-order, are $b_c\delta_l = 3, 2.27, 2.05$. The exact $\Omega = 1$ solution is $b_c = a_c = 1.69$; it can be appreciated that the results converge to the exact value: the difference is reduced from 1.31 to .36. Other cosmologies lead to very similar values of b_c , which differ from by not more than 3 per cent (Lilje 1992). For the Lagrangian perturbation scheme, spherical symmetry is the hardest to deal with, so we expect faster convergence in more general cases (see the discussion in M95).

The first-order solution for general ellipsoids is simply $b_c^{(1)} = 1/\lambda_1$; it has been amply discussed in M95 (note that, due to the different signs of the λ_i eigenvalues, b_c was $-1/\lambda_3$ in M95). The second-order solution for initially overdense ellipsoids is:

$$b_c^{(2)} = \frac{7\lambda_1 - \sqrt{7\lambda_1(\lambda_1 + 6\delta_l)}}{3\lambda_1(\lambda_1 - \delta_l)}. \tag{12}$$

If $\delta_l < 0$, the second-order equation gives meaningful solutions only if $\delta_l \geq -\lambda_1/6$, i.e. only for relatively small underdensities. Other solutions exist which make even a spherical void collapse! These had already been noted by Sahni & Shandarin (1996), and show how the 2nd-order Lagrangian scheme is unreliable for initially underdense perturbations. The reason for this behaviour is that 2nd-order perturbations, being of even order, do not properly recognize voids, making them collapse.

The third-order solution is the smallest non-negative solution of the equation:

$$\begin{aligned}
1 - \lambda_1 b_c^{(3)} - \frac{3}{14}\lambda_1(\delta_l - \lambda_1)(b_c^{(3)})^2 \\
- \left(\frac{\mu_3}{126} + \frac{5}{84}\lambda_1\delta_l(\delta_l - \lambda_1)\right)(b_c^{(3)})^3 = 0,
\end{aligned} \tag{13}$$

where $\mu_3 = \lambda_1\lambda_2\lambda_3$. Though it is not straightforward to choose analytically the right root of this equation, it is very easy to find it with a computer. The third-order equation gives meaningful solutions also for initially underdense elements, thus avoiding the problems encountered with the second-order solutions. This shows that third-order pertur-

bation theory is necessary when predicting the instant of collapse of general mass elements.

Both at second and third-order, the first axis to collapse is the one corresponding to the largest λ eigenvalue, λ_1 ; this is by itself an indication of convergence, as it means that the first-order (Zel'dovich) approximation, which predicts collapse first on the 1-axis, makes the greatest contribution to collapse dynamics.

The calculations of the exact collapse time of the ellipsoid have been performed as in M95; the equations are reported in Appendix B. To improve the calculations, the integration has been divided into two parts: after decoupling, defined as the instant when the density starts to grow, the integration variable has been changed from (logarithm of) b to (logarithm of) the density; the integration has been stopped at $\delta = \exp(15)$. This had led to a modest but appreciable improvement in precision. The precision of the calculation depends on the initial conditions: the spherical collapse is predicted with a precision of around 0.2 per cent, while the 'pancake' collapse, when $\lambda_2 = \lambda_3 = 0$, is recovered with a precision of 8 per cent. The calculations have been performed only for $\delta_l = 1$ or -1 ; the other cases can be found by using the scaling relation:

$$b_c(\lambda_1, \lambda_2, \lambda_3) = kb_c(k\lambda_1, k\lambda_2, k\lambda_3). \tag{14}$$

Figs. 1a, b and c show the various b_c curves of initially overdense and underdense ellipsoids. The x and y variables, which range from 0 to ∞ , are defined as $x = \lambda_1 - \lambda_2$, $y = \lambda_2 - \lambda_3$; they give a measure of the initial shear of the ellipsoid (see M95). A number of things can be noted:

- (i) The predictions at increasing Lagrangian orders always converge to the exact value (within the numerical errors quoted above); in the initial underdensity case, only the odd Lagrangian orders converge to the solutions.
- (ii) The convergence is very fast for large shears; in this case (for initially overdense ellipsoids), the third-order solution does not much improve the agreement with the numerical solution, with respect to the second-order one.
- (iii) Initially underdense ellipsoids can collapse if the shear is large enough; in this case the third-order prediction is always sufficiently accurate.

These results can be used to predict the collapse time of a homogeneous ellipsoid in a fast and accurate way (probably more accurate than numerical integration). It is necessary to correct the second- and third-order predictions in order to reproduce the correct behaviour in the quasi-spherical overdense cases. This correction can be expressed in the following way:

$$b_c^{(nC)} = b_c^{(n)} - \Delta \exp(-ax - by), \tag{15}$$

where $n=2,3$, and the three coefficients take on the following values:

	2nd ord	3rd ord	
$\Delta =$	0.580	or 0.364	(16)
$a =$	5.4	or 6.5	
$b =$	2.3	or 2.8	

This corrections are applied only when $\delta_l > 0$; no correction is applied when $\delta_l \leq 0$.

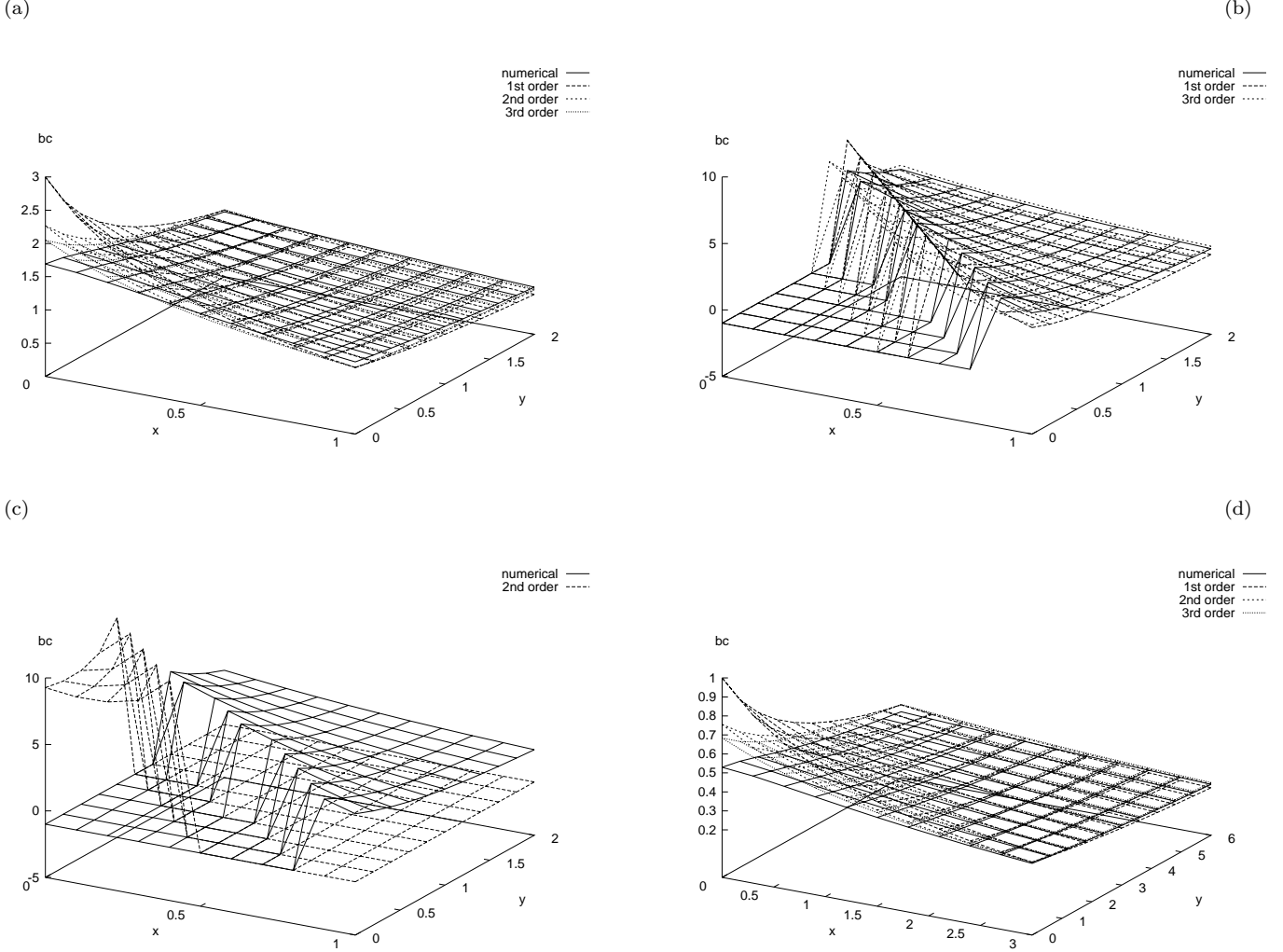


Figure 1. Collapse times b_c of homogeneous ellipsoids according to Lagrangian perturbation theory, compared with a numerical integration; $x = \lambda_1 - \lambda_2$ and $y = \lambda_2 - \lambda_3$. (a): initial overdensity $\delta_l = 1$. (b) and (c): initial underdensity $\delta_l = -1$; 2nd-order predictions have been put in a separate figure for the sake of clarity. (d): open universe, initial overdensity $\delta_l = 3$; the Ω dependence of the time functions is neglected.

All these calculations have been repeated with two other background models, namely the open $\Omega_0 = 0.2$ model and the flat $\Omega_0 = 0.2$ model with cosmological constant. The Lagrangian calculations are quite insensitive to the cosmology, as shown by equations (A7) (note that the pancake case, $x = \delta_l$ and $y = 0$, being exactly predicted by Zel'dovich, is always independent of the cosmology). As expected, the numerical calculations give very similar results for the b_c function, with slightly larger errors when the background density becomes small and the ellipsoid takes a long time to collapse. Fig. 1d shows the $\Omega = 0.2$ case; an initial overdensity $\delta_l = 3$ has been chosen to allow the collapse of all the ellipsoids reproduced in the figure. Then, the above-mentioned results for b_c can be used in any of the cosmologies checked here.

In conclusion, the Lagrangian series can be used to accurately approximate the collapse of a homogeneous ellipsoid. On the other hand, homogeneous ellipsoid collapse can be seen as a particular truncation of the Lagrangian series. Its ability to reproduce the collapse time of generic perturba-

tions will be shown in the next section. In this case, ellipsoidal collapse has to be considered not as a description of the dynamics (or even the geometry!) of an *extended* region, but as an approximate description of the *local* dynamics of a mass element.

Before going on, it is useful to comment on the concept of 'locality'. From a mathematical point of view, the evolution of a continuous system is local if its evolution equations are ordinary differential equations, i.e. with no partial derivatives*. Thus, any point's trajectory is fully determined by its initial conditions, i.e. it is not necessary to evolve all the trajectories together. From a physical point of view, non-locality can be associated to the long-range character of gravitational forces: the fate of a mass element depends on all the other mass elements. The non-local character of gravitational dynamics has recently been stressed again in a

* It is assumed that there is no explicit coupling between field values at different points

paper by Kofman & Pogosyan (1995). Nonetheless, some dynamical approximations predict ‘local’ dynamical evolution. The unrealistic spherical model is such a one: the fate of a spherical perturbation depends only on its initial density. At variance, the Zel’dovich approximation gives some information on non-local tidal forces: the motion of a mass element depends on all other elements. This information is contained in the gravitational potential, which is related to the density by a non-local Poisson equation. Thus the Zel’dovich approximation is physically non-local. But, once the initial peculiar potential is known, the dynamical evolution is local, in the mathematical sense given above. In other words, the initial conditions contain non-local information, while the evolution is local. The same holds true for the homogeneous ellipsoidal collapse model. Analogous considerations can be applied to the Lagrangian perturbation theory at any order, as the equations for the perturbative terms are separable in space and time, as recently demonstrated by Ehlers & Buchert (1996). If this is the case, the non-local space equations (A13) give non-local initial conditions, while the subsequent dynamics is independently determined for every single trajectory. But, while it is relatively simple to obtain the statistical distribution of the initial conditions for the Zel’dovich approximation, namely of the λ_i eigenvalues, the analytical determination of the statistical distribution of other contributions leads to discouraging mathematical difficulties. Nonetheless, as a consequence of the mathematical ‘locality’ of Lagrangian perturbations, the perturbative terms have to be calculated just once at the beginning, making this kind of calculation dramatically faster than usual N-body simulations.

5 COLLAPSE TIME IN THE GAUSSIAN FIELD CASE

In this section, Gaussian fields with scale-free power spectra are considered. To proceed analytically, the equation $J = \det(\delta_{ab} + S_{a,b}) = 0$ ought to be solved for general initial potentials, and the probability distribution function (hereafter PDF) of its smallest non-negative root ought to be obtained. As a matter of fact, it is very hard to get the whole PDF of the various contributions to the deformation tensor. Even neglecting the non diagonalizable 3c term, the various contributions to $S_{a,b}$ are not diagonal in the same frame. It is definitely convenient to get the PDF of the collapse times by constructing realizations of Gaussian fields in cubic grids.

In these calculations the grid does not need to be very large: what is needed is a sufficient degree of non-locality, which is provided even by small grids. 16^3 and 32^3 grids have been used, with identical results. Initial potentials have been simulated, following what is done for initial conditions of N-body simulations. Power spectra have been chosen as $P_\varphi(k) \propto k^{n-4}$, with $n = -2, -1, 0$ and 1 ; these correspond to matter perturbation spectra $P_\delta(k) \propto k^n$. Spectra have been normalized with $\sigma = 1$, where σ is the total density variance. Of course, any other normalization can be obtained by a time rescaling.

Ten realizations have been performed for every power spectrum. Poisson equations (A13) have been solved with Fast Fourier Transform (FFT) techniques; FFT have also

been used to calculate the derivatives of the various potentials. The growing mode b has been used as a time variable, and the Ω dependence of the time functions b_n (equations A7) has again been neglected. The following collapse time estimates have been calculated for every point: spherical collapse (hereafter SPH), 1st-order or Zel’dovich approximation (1ST), 2nd-order (2ND), 3rd-order (3RD) and ellipsoidal collapse (ELL). SPH, 1ST and ELL collapse times have been calculated analytically, on the basis of the λ eigenvalues of $\varphi_{,ab}$ at any point; ELL has been calculated at third-order and corrected around the spherical value as in equation (15). 2ND and 3RD have been calculated by looking for the instant at which $J < 0$, then using conventional root-finding algorithms. It is possible that J becomes negative and then positive soon after; these events can be lost if the search is not fine enough. As a matter of fact, a very small number of points, on the order of a few times 10^{-5} of the total number, were missed by the searching algorithm.

Buchert, Melott & Weiß (1994) state that third-order terms are very sensitive to numerical calculations. The same thing has been found in these analyses; third-order calculations are not expected to be very precise. This has been noted especially for the transversal 3c contribution. Anyway, that contribution has been found not to influence the collapse time appreciably, so it has been neglected in the calculations.

From every set of 10 realizations, nearly 10000 points have been randomly extracted to analyze the statistics of collapse times. Figs. 2a-j and 3a-j show the scattergrams of the five collapse estimates, for $n = -2$ and $n = 1$. Points which are predicted not to collapse have been assigned a small negative collapse time, -0.1. Then, the points which are predicted to collapse according to one prediction, but not according to the other, are recognizable in the scattergrams as horizontal or vertical rows of points. These points will be called *discordant* in the following. Mean values and dispersions around the bisector of non-discordant points are superimposed on the scattergram. Finally, Figs 2 and 3 focus on the interesting zone $b_c < 3$, which includes the points forming the large-mass part of the MF.

Many conclusions can be drawn from Figs. 2 and 3:

(i) As expected, SPH correlates with the other predictions for the fastest collapsing points (in agreement with Bernardeau 1994), but it badly overestimates the collapse time in general cases; moreover, many points (those with $\delta_l < 0$!) are incorrectly not predicted to collapse. Then, non-locality strongly accelerates collapse with respect to the spherical case, in line with the conclusions of M95. As a conclusion, spherical collapse is not suitable, even statistically, for describing gravitational collapse.

(ii) The 1ST – 2ND and the 2ND – 3RD correlations at small collapse times are increasingly good (though the former has a considerable scatter); this demonstrates the convergence of the Lagrangian series in predicting the collapse time of the fast collapsing points. The 1ST – 3RD correlation is similar to that of 1ST – 2ND.

(iii) The discordant points in the 2ND – 3RD scattergram are either some initially slightly non-negative ones, for which 2ND does not find any solution, as in the ellipsoidal case, (and then $b_c^{(2ND)} = -0.1$), or voids which are incorrectly predicted to collapse by 2ND (and then $b_c^{(3RD)} = -0.1$). This

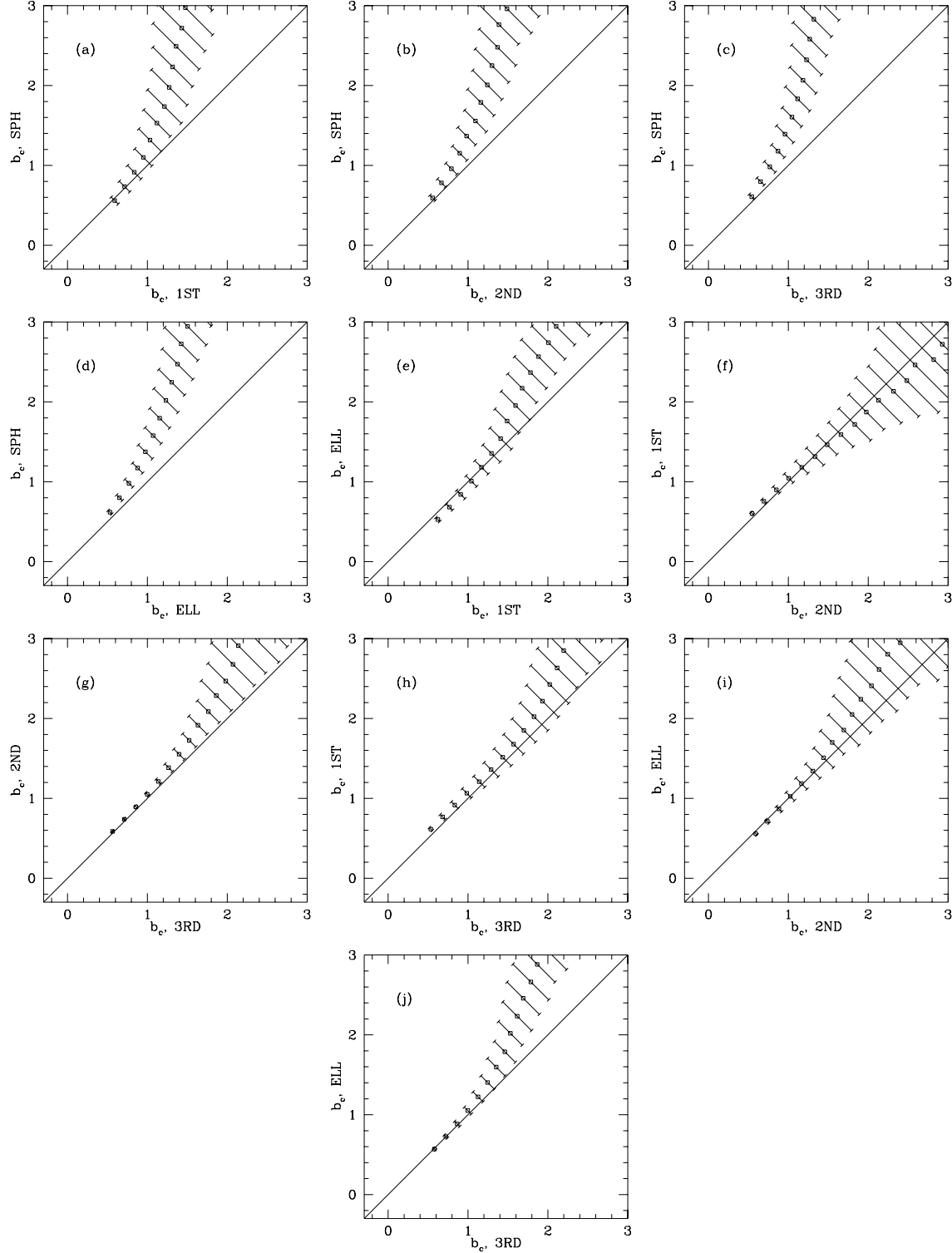


Figure 2. Scattergrams of the various collapse time estimates b_c , for a Gaussian field with $n = -2$.

shows the necessity of third order calculations for the collapse time. The same features are recognizable in the other 2ND scattergrams. (N.B. The very small number of discordant points, less than 10 in 10000, which collapse according to 1ST and ELL, but not according to 3RD, are the ones

missed by the algorithm which looks for $J = 0$; see the discussion above.)

(iv) 3RD accelerates the collapse of the points with $b_c > 1$ with respect to all the other predictions. Given the uncertainties connected with third-order calculations, this feature is not considered very robust. Moreover, 3RD predicts the

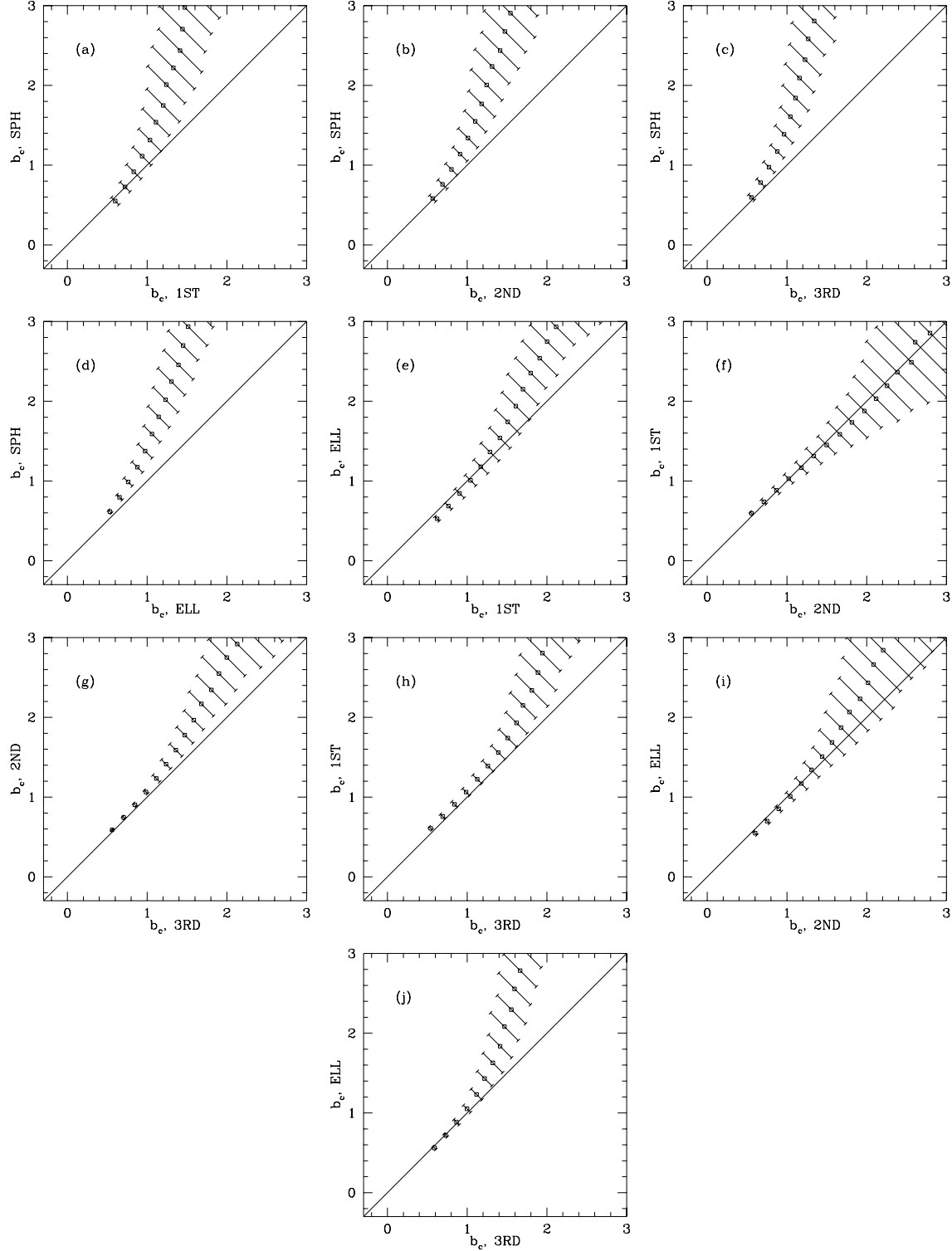


Figure 3. Scattergrams of the various collapse time estimates b_c , for a Gaussian field with $n = 1$.

collapse of more points than 1ST. Again it is not clear at all if this feature, regarding points completely outside of the convergence range of the Lagrangian series, has some meaning. Probably Lagrangian perturbations are not a good means for determining the fraction of collapsed mass in a smooth universe.

(v) ELL shows an encouraging correlation with 2ND and an even better one with 3RD, when b_c is small. Note how 1ST, 2ND and 3RD, when b_c is small, converge to a solution which tightly correlates with ELL. This has two implications, namely that the Lagrangian series probably converges to the true solution and that ELL can be used as a realis-

tic estimate of the collapse time. Moreover, ELL tends to underestimate the collapse time for $b_c > 1$, slightly with respect to 2ND and strongly with respect to 3RD. This would mean that the non-locality not contained in the ELL estimate speeds up the collapse.

(vi) The results are essentially independent of n ; the weak differences that can be visible in the scattergrams will be quantified in the following.

These results are strictly correct for an Einstein de-Sitter Universe, in which case the scale factor can be used as a time variable, $b_c = a_c$. Due to the very weak Ω -dependence of the time functions, when expressed in terms of b , the results for $\Omega \neq 1$ cosmologies are nearly indistinguishable. The most important effect, in the open case, is that the growing mode saturates at the value $b = 5/2$; a mass element with that collapse “time” collapses at an infinite physical time, and larger b_c imply no collapse.

As noted in Section 4, ELL can be considered as a truncation of the Lagrangian series, or, better, of its ‘local forms’. It is interesting to check whether the use of the full local forms of the Lagrangian series improves the agreement of the approximation to the complete calculation. Here only the second-order terms will be considered; in this case, 2nd-order local and ellipsoidal displacements are equal, the differences come into the deformation tensor. The 2nd-order deformation tensor, its local and its ellipsoidal parts have been calculated for every point of a 16^3 realization with power spectrum $n = 0$. Fig. 4 shows the scattergrams of one of the diagonal elements of the 2ND deformation tensor, $S_{1,1}^{(2)}$ versus its local form, $S_{1,1}^{(2L)}$, and its ellipsoidal part, $S_{1,1}^{(2E)}$. Fig. 4 also shows the same pictures for one of the off-diagonal elements; other diagonal and off-diagonal elements obviously behave identically. The local diagonal elements correlate with the 2ND ones just slightly better than the ellipsoidal ones, while no correlation of the off-diagonal terms is visible in any case. Fig. 5 shows the corresponding collapse times; here the ellipsoidal collapse time is given by equation (12), without any correction. Again, the ellipsoidal part reproduces the full 2ND collapse time nearly as well as the local form. As a conclusion, it is convenient to truncate the local forms as in Section 4, as it leads to a great simplification of the calculations and to a similar agreement with the full Lagrangian terms.

5.1 The inverse collapse time PDF

To quantify the PDF of the collapse times, it is convenient to consider their inverses, as they are better behaved: the inverse collapse times are large, but of order one, for fast collapsing points, and become smaller and smaller for slowly collapsing ones; the passage from collapse to non collapse is not at infinity, as for b_c , but at 0. We define:

$$F(\mathbf{q}) = b_c^{-1}(\mathbf{q}). \quad (17)$$

In the SPH case, $F = \delta_l/1.69$; in the 1ST case, $F = \lambda_1$. This definition is also convenient for determining the MF (see paper II).

Fig. 6 shows both the cumulative and differential F PDFs for $n = -2$ and 1; the cumulative curves give a binning-free picture of the PDFs, while the differential ones,

in logarithmic scale, better exhibit the behaviour in the rare event tail. The following things can be noted:

(i) The SPH curve is quite different from all the others, even at the high F tail: as in M95, a systematic departure from spherical collapse influences also the statistics of rare events.

(ii) In the range $F \geq 1$, the 1ST, 2ND and 3RD curves show a monotonic shift toward large F values, which can be interpreted as convergence toward a solution. This is not true for $F < 1$; the bad behaviour of 2ND in initial underdensities is the probable cause.

(iii) ELL and 3RD nearly coincide down to $F = 1.2$, which corresponds to $b_c = 0.83$, and overall have a similar behaviour; ELL slightly makes more mass collapse at large F values, because 3RD slightly underestimates quasi-spherical collapses. The main differences come out in the range where the convergence of the Lagrangian series is not guaranteed, but both 1ST, 2ND and 3RD have larger medians than ELL; so ELL probably underestimates the collapses around $F = 0.5$ or $b_c = 2$.

(iv) The n dependence can be appreciated in Fig. 6. As expected, SPH, 1ST and ELL are essentially independent of n (the λ_i distribution is fixed once the mass variance is fixed), while the n dependence of 2ND and 3RD is weak. Moreover, the difference between ELL and 3RD is smaller for smaller n , i.e. when more large-scale power is present, while we would expect the opposite if the difference of 3RD from ELL were due to non-locality induced from large scales. In the following the weak n -dependence of 3RD will be neglected.

(v) The range $F > 1$, where the Lagrangian series converges to ELL, corresponds to more than 10 per cent of the points, i.e., of the mass. 20 per cent of the mass is found in $F > 0.8$, where ELL and 3RD are not very different, while all the medians can be found around $F \sim 0.5$. So the convergence of the Lagrangian series and its agreement with ELL take place for a significant quantity of mass, covering more than the large-mass tail of the MF, while the appreciable differences between ELL and 3RD affect the power-law part of the MF, which is plagued by a number of other problems (see paper II).

To calculate the MF, an analytical expression for the F PDF is needed. To find it, it is useful to look for a coordinate transformation which maps the given PDF to a Gaussian one, with zero mean and unit variance. Consider then the quantity F with its PDF $P_F(F)$, and a normal Gaussian $P_G(x) = \exp(-x^2/2)/\sqrt{2\pi}$. If the function P_F is well-behaved enough, a transformation $x(F)$ will exist such that:

$$P_F(F)dF = P_G(x(F))dx(F) = \frac{1}{\sqrt{2\pi}}e^{-x(F)^2/2}dx(F). \quad (18)$$

The function $x(F)$ can be found as a solution of the ordinary differential equation:

$$\frac{dx(F)}{dF} = \sqrt{2\pi}P_F(F)\exp\left(\frac{x(F)^2}{2}\right). \quad (19)$$

This equation can be easily solved with a computer. The initial condition of the equation is best set by integrating from the median of the P_F distribution, setting $x(F) = 0$ at that point.

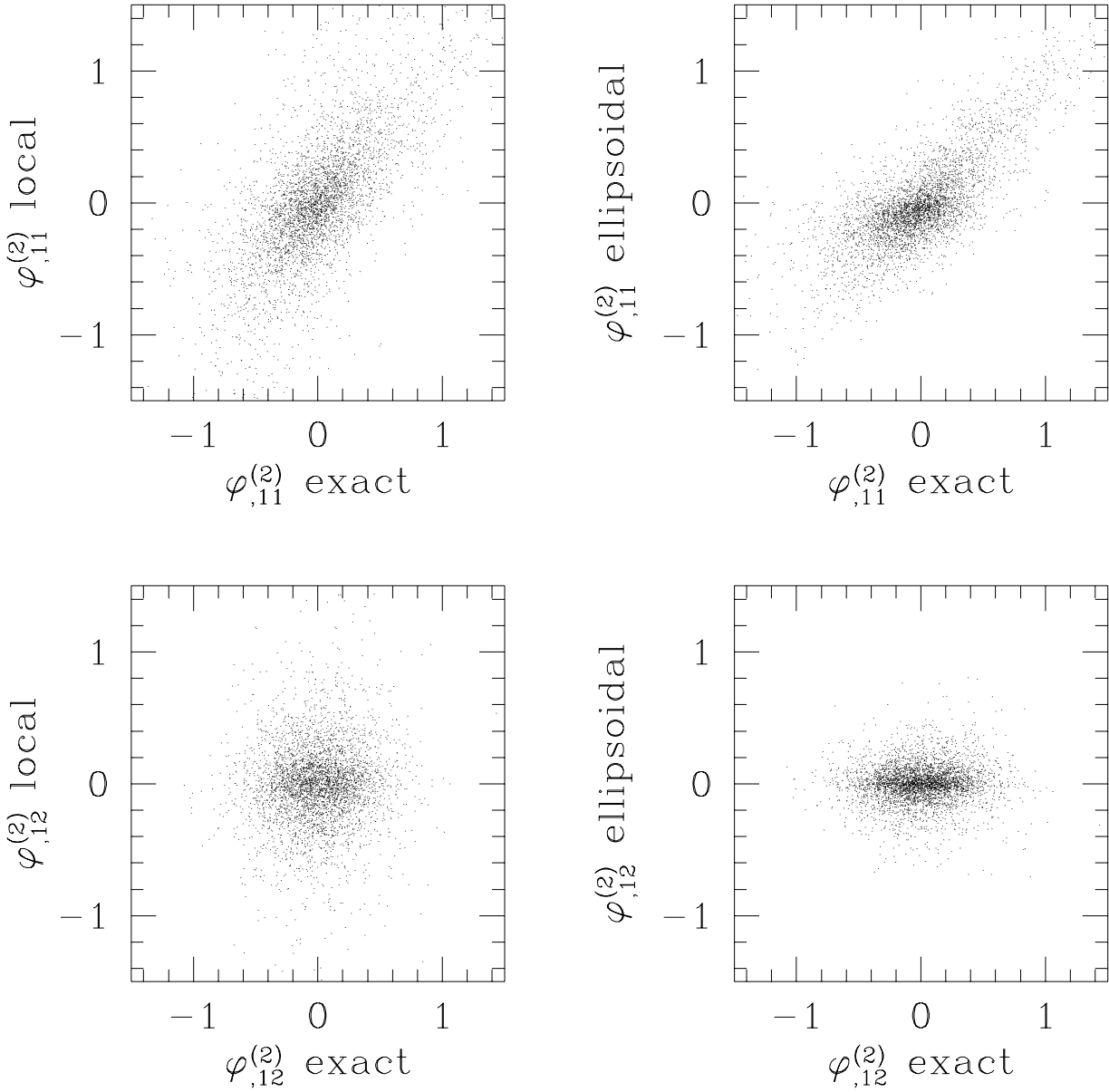


Figure 4. Scattergrams of diagonal ($\phi_{,11}$) and non-diagonal ($\phi_{,12}$) matrix elements of the 2nd-order contributions to the deformation tensor, calculated either exactly or by using local forms or their ellipsoidal parts.

Equation (19) has been solved for the ELL and 3RD distributions. The 3RD distribution has been mediated over the four spectral indexes considered, so as to neglect the n dependence. The results are shown in Fig. 7a: in both cases the transformations for $F > 1$ are accurately linear, i.e. the large- F parts of the F distributions are Gaussians. (Note that the weak rise of the $x(F)$ curve in the large- F end is an artifact). The $x(F)$ transformations are accurately fit by the following expressions:

$$x(F)_{ELL} = -0.69 + 1.82F - 0.4(\text{erf}(-7.5F + 1.75) + 1) \quad (20)$$

$$x(F)_{3RD} = -1.02 + 2.07F - 0.75(\text{erf}(-3F + 1.18) + 1) ;$$

these analytical fits do not reproduce well the $x(F)$ curves for $F < 0.2$; on the other hand, that part of the PDFs is very uncertain. The first two terms represent the linear fits, valid for large F values. Fig. 7b shows the two ELL and 3RD PDFs, together with their Gaussian (coming from the linear transformations) and non-Gaussian (coming from the complete transformation) fits. Both non-Gaussian distributions, compared with the Gaussian ones, show a peak at small F ; the two peaks have similar heights but slightly different positions. These correspond to the falling tail in the transformation curves $x(F)$.

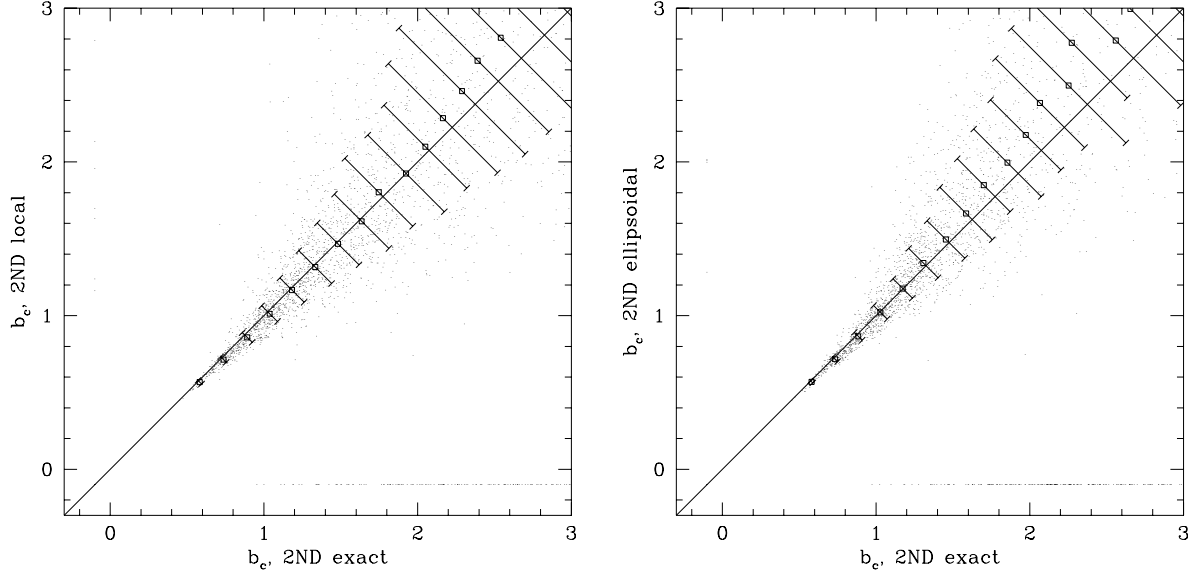


Figure 5. Scattergrams of 2ND collapse time estimates b_c , calculated either exactly or by using local forms or their ellipsoidal parts.

6 SUMMARY AND CONCLUSIONS

In this paper, the dynamical part of a new theory of the mass function of cosmic structures has been presented. An accompanying paper, paper II, develops the statistical machinery necessary to calculate the MF. The key point of all the dynamical analysis is the use of a fluidodynamical Lagrangian framework to predict the fate of a mass element of a smooth field. The Lagrangian perturbative scheme has been used to approximate the real dynamics of the smoothed cosmological fluid up to orbit crossing. The strongest hypothesis of the whole theory is that small-scale structure does not influence the dynamics of larger collapsing scales. The OC instant has been chosen as suitable definition of collapse of a mass element. This definition has been amply discussed.

To check the performances of Lagrangian perturbations in predicting the OC instant, when all the terms of the series are of the same order, the collapse of a homogeneous ellipsoid has been considered. The Lagrangian series converges fast in predicting the collapse of a homogeneous ellipsoid, except for quasi-spherical ones; a simple correction can be applied in this case. Third-order terms are necessary to give good collapse estimates of initial underdensities. On the other hand, ellipsoidal collapse can be considered as a truncation of the *whole* Lagrangian series. In this case, as in M95, ellipsoidal collapse has to be considered an approximation of the local collapse of a point mass, not of an extended region of approximate ellipsoidal shape.

The collapse of scale-free Gaussian fields simulated on a 32^3 grid has been considered. The Lagrangian series has been found to clearly converge to a solution for the fast-collapsing points, about 10 per cent of the total mass. Approximate convergence has been observed for about 50 per cent of the mass. The homogeneous ellipsoidal model has been found to strongly correlate with the third-order Lagrangian collapse in the same range of validity. The ellipsoidal model can thus be used as a fast and easy to implement approximation of collapse dynamics. The spherical

model, instead, has been found to behave differently from the other predictions. The inverse collapse-time distributions have been calculated for the third-order Lagrangian and ellipsoidal predictions. These will be necessary for determining the MF.

With this dynamical description of collapse, it is possible to construct a MF, fully based on realistic dynamics. The role of the initial density is taken by the inverse collapse time F . This quantity is by no means a Gaussian process, but is a complicated non-linear functional of a parent Gaussian process. This introduces a number of complications in the statistical treatment of the MF, which will be faced in paper II.

The following points, raised by the analysis presented here, are relevant when constructing a MF:

- (i) As the main quantity, F , is (the inverse of) a time, any threshold F_c in this theory simply specifies the time at which the MF is examined; there is no free δ_c parameter.
- (ii) The dynamical predictions are strictly punctual; in other words, a point collapses if it is predicted to collapse (at a given scale), not if a neighboring collapsing point is able to involve it in its collapse.
- (iii) Smoothing is necessary because of the truncated nature of the dynamical approximations used. Thus the shape of the filter has to be chosen in order to optimize the performances of the dynamical predictions; usually Gaussian filters are suggested.

The collapse time, which is needed to determine the MF, is not the only information one can obtain on a collapsing mass element. In practice, all the trajectories of the collapsing points are known. This has the consequence that much more than a MF can be calculated. A possible application is the determination of the angular momentum of a collapsing region; Lagrangian perturbation theory is an appropriate framework for estimating such a quantity, as Catelan & Theuns (1996a,b) have recently shown. The rich-

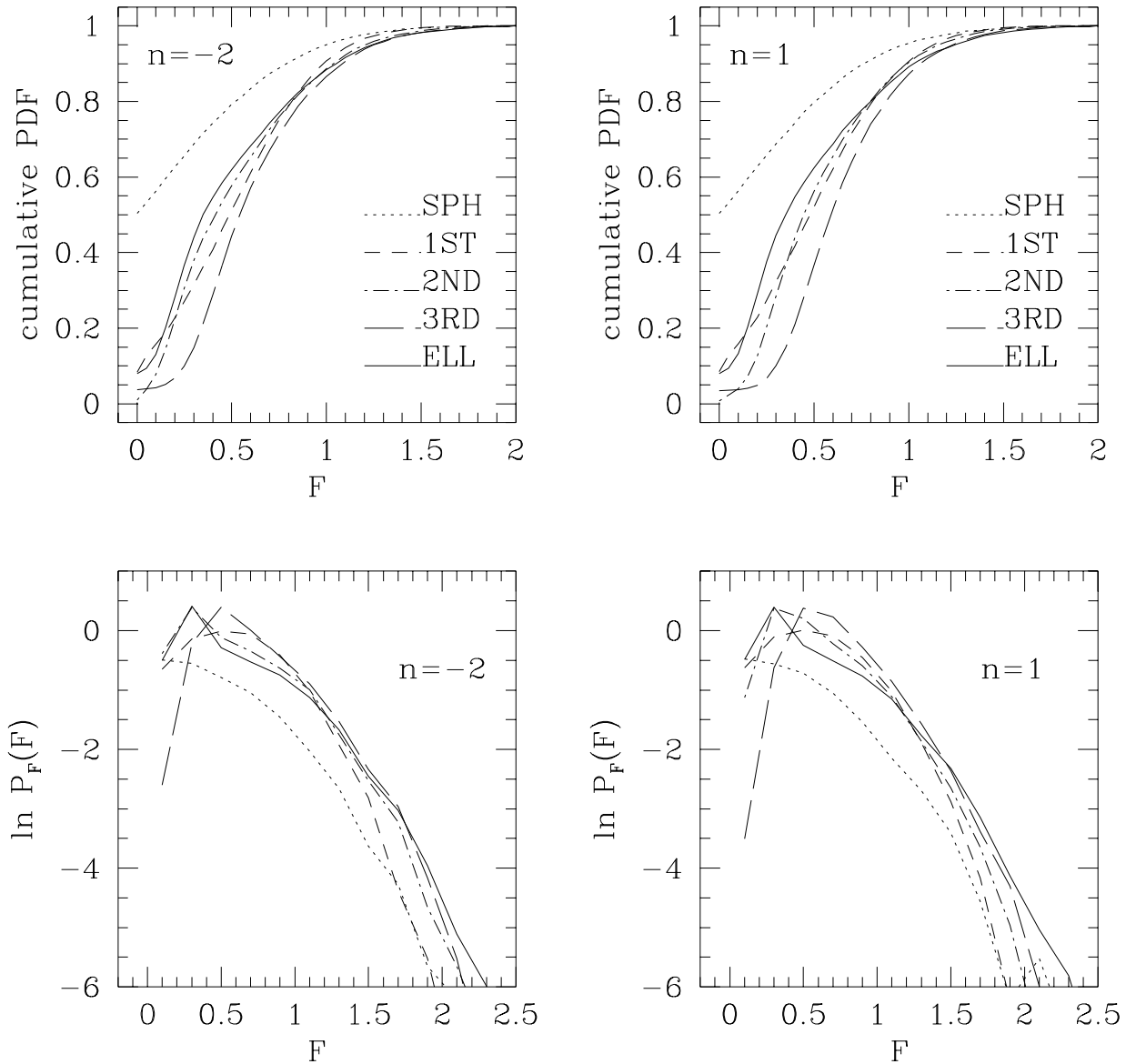


Figure 6. Cumulative and differential PDF of various inverse collapse time estimates F , for $n = -2$ or $n = 1$.

ness of the dynamical information makes it possible to put further dynamical constraints on the collapsing regions, if special classes of objects are required.

To finally decide on the validity of the MF dynamics presented here, the predictions of this theory have to be tested against N-body simulations. As collapsed regions are defined to coincide with orbit-crossed regions, they have to be sought for by a suitable algorithm; equation (8) could provide such an algorithm. This MF is expected to carefully reproduce the N-body MF as long as Lagrangian perturbation theory is expected to give a correct description of collapsing dynamics, i.e. for large masses, comprising at least 10-20 per cent of mass, and when few small-scale structures are present, i.e. with small spectral indexes.

ACKNOWLEDGMENTS

I wish to thank Alfonso Cavaliere and Sabino Matarrese for a number of discussions and for their encouragement. I also thank Thomas Buchert and Paolo Catelan for discussions on the Lagrangian perturbation theory, and an anonymous referee for its suggestions which have been of great help in improving the presentation. This work has been partially supported by the Italian Research Council (CNR-GNA) and by the Ministry of University and of Scientific and Technological Research (MURST).

REFERENCES

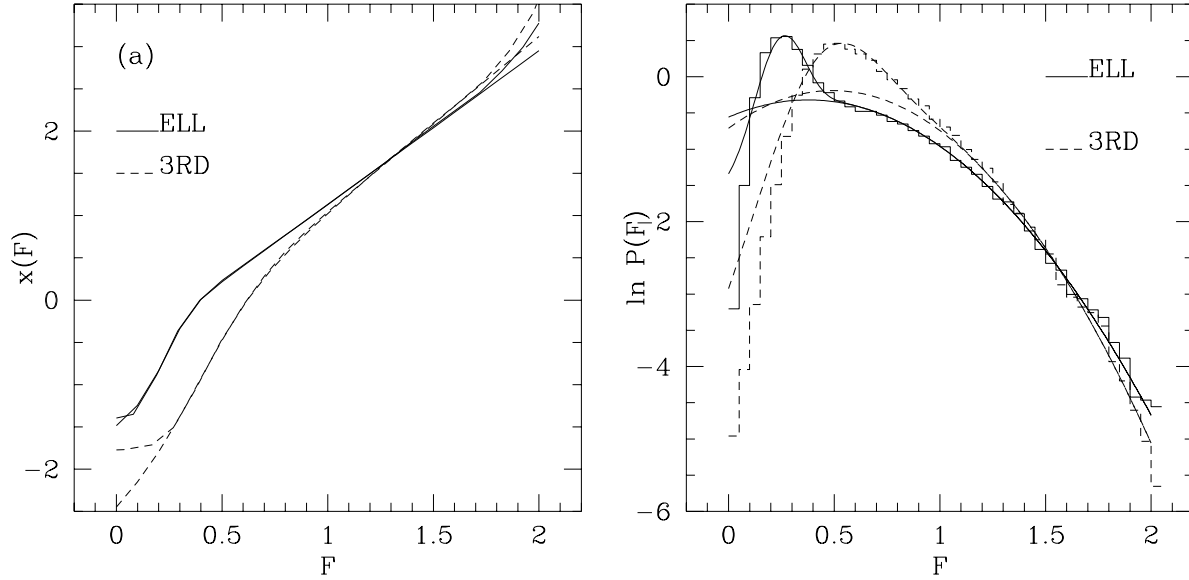


Figure 7. (a): Heavy lines: transformations of variable $x(F)$ which make the ELL or 3RD F PDFs Gaussian. Light lines: analytical approximations. (b): Histograms of 3RD and ELL F PDFs, with their Gaussian and complete analytical approximations.

Ashman K.M., Salucci P., Persic M., 1993, MNRAS, 260, 610
 Audit E., Alimi J.M., 1996, submitted to A&A (astro-ph 9609156)
 Bahcall N.A., Cen R., 1993, ApJ, 407, L49
 Bernardeau F., 1994, ApJ, 427, 51
 Biviano A., Girardi M., Giuricin G., Mardirossian F., Mezzetti M., 1993, ApJ, 411, L13
 Bond J.R., Cole S., Efstathiou G., Kaiser N., 1991, ApJ, 379, 440
 Bond J.R., Myers S.T., 1996, ApJS, 103, 1
 Bouchet F.R., 1996, in Bonometto S., Primack J., Provenzale A., eds., Dark Matter in the Universe. In press (astro-ph 9603013)
 Bouchet F.R., Colombi S., Hivon E., Juszkiewicz R., 1995, A&A, 296, 575
 Bouchet F.R., Juszkiewicz R., Colombi S., Pellat R., 1992, ApJ, 394, L5
 Bower R.G., 1991, MNRAS, 248, 332
 Buchert T., 1989, A&A, 223, 9
 Buchert T., 1992, MNRAS, 254, 729
 Buchert T., 1994, MNRAS, 267, 811
 Buchert T., 1996, in Bonometto S., Primack J., Provenzale A. eds., Dark Matter in the Universe. In press (astro-ph/9603013)
 Buchert T., Ehlers J., 1993, MNRAS, 264, 375
 Buchert T., Karakatsanis G., Klaff R., Schiller P., 1997, A&A, in press (astro-ph/9510133)
 Buchert T., Melott A.L., Weiß A.G., 1994, A&A, 288, 349
 Catelan P., 1995, MNRAS, 276, 115
 Catelan P., Theuns T., 1996a, MNRAS, 282, 436
 Catelan P., Theuns T., 1996b, MNRAS, 282, 455
 Cavaliere A., Menci N., Tozzi P., 1994, in Seitter W.C., ed., Cosmological Aspects of X-ray Clusters of Galaxies. Kluwer Ac. Pub., Dordrecht
 Cavaliere A., Menci N., Tozzi P., 1996, ApJ, 464, 44
 Coles P., Melott A.L., Shandarin S.F., 1993, MNRAS, 260, 765
 Ehlers J., Buchert T., 1997, GRG, in press (astro-ph/9609036)
 Eisenstein D.J., Loeb A., 1995, ApJ, 439, 520
 Fort B., Mellier Y., 1994, A&A Rev., 5, 239
 Gurbatov S.N., Saichev A.I., Shandarin S.F., 1989, MNRAS, 236, 385
 Henry J.P., Arnaud K.A., 1991, ApJ, 372, 410
 Kofman L., Pogossyan D., 1995, ApJ, 442, 30

Lacey C., & Cole S., 1993, MNRAS, 262, 627
 Lacey C., & Cole S., 1994, MNRAS, 271, 676
 Lachièze-Rey M., 1993a, ApJ, 407, 1
 Lachièze-Rey M., 1993b, ApJ, 408, 403
 Lilje P.B., 1992, ApJ, 386, L33
 Lucchin F., Matarrese S., 1988, ApJ, 330, 535
 Matarrese S., Lucchin F., Moscardini L., Saez D., 1992, MNRAS, 259, 437
 Melott A.L., Buchert T., Weiß A.G., 1995, A&A, 294, 345
 Monaco P., 1995, ApJ, 447, 23 (M95)
 Monaco P., 1996, submitted to MNRAS (astro-ph/9606029) (paper II)
 Moutarde F., Alimi J.M., Bouchet F.R., Pellat R., Ramani A., 1991, ApJ, 382, 377
 Peacock J.A., Heavens A.F., 1990, MNRAS, 243, 133
 Pisani A., Giuricin G., Mardirossian F., Mezzetti M., 1992, ApJ, 389, 68
 Porciani C., Ferrini F., Lucchin F., Matarrese S., 1996, MNRAS, 281, 311
 Press W.H., Schechter P., 1974, ApJ, 187, 425 (PS)
 Press W.H., Teukolsky S.A., 1990, Computers in Physics Jan/Feb, 1990, 92
 Sahni V., Coles P., 1995, Phys. Rep., in press (astro-ph/9505005)
 Sahni V., Shandarin S.F., 1996, MNRAS, 282, 641
 Shandarin S.F., Zel'dovich Ya.B., 1989, Rev. Mod. Phys., 61, 185
 Shaviv N.J., Shaviv G., 1995, ApJ, 448, 514
 Sheth R.K., 1996, MNRAS, 261, 1277
 Vergassola M., Dubrulle B., Frisch U., Noullez A., 1994, A&A, 289, 325
 Yano T., Nagashima M., Gouda N., 1996, ApJ, 466, 1
 Zel'dovich Ya.B., 1970, Astrofizika, 6, 319 (transl.: 1973, Astrophysics, 6, 164)

APPENDIX A: LAGRANGIAN PERTURBATIONS

This appendix contains a number of technical points on Lagrangian perturbation theory.

Peculiar velocity, acceleration and density contrast of a mass element can be written in terms of the \mathbf{S} field as:

$$\begin{aligned} \mathbf{v}(\mathbf{q}, t) &= a(t)d\mathbf{S}(\mathbf{q}, t)/dt \\ \mathbf{g}(\mathbf{q}, t) &= a(t)d^2\mathbf{S}(\mathbf{q}, t)/dt^2 + 2H\mathbf{v}(\mathbf{q}, t) \\ 1 + \delta(\mathbf{q}, t) &= J(\mathbf{q}, t)^{-1}[1 + \delta(\mathbf{q}, t_0)] ; \end{aligned} \quad (\text{A1})$$

here $\mathbf{v}(\mathbf{q}, t)$ is the peculiar velocity of the element \mathbf{q} , $\mathbf{g}(\mathbf{q}, t)$ is its peculiar acceleration, δ its density, d/dt denotes total (Lagrangian) time derivative, $a(t)$ is the scale factor of the background cosmology, $H = a^{-1}da/dt$ is the Hubble parameter, t_0 is an initial time and $J(\mathbf{q}, t)$ is the Jacobian determinant, equation (3).

The evolution equations for the displacement field \mathbf{S} can be written, following Catelan (1995), as:

$$[(1 + \nabla \cdot \mathbf{S})\delta_{bd} - S_{b,d} + S_{b,d}^C]\ddot{S}_{a,d} = \alpha(\tau)[J - 1] \quad (\text{A2})$$

$$\varepsilon_{abc}[(1 + \nabla \cdot \mathbf{S})\delta_{bd} - S_{b,d} + S_{b,d}^C]\dot{S}_{c,d} = 0 , \quad (\text{A3})$$

where the dot denotes the Lagrangian derivative with respect to the time variable $\tau = t^{-1/3} = a^{-2}$, if $\Omega_0 = 1$, or

$$\tau = |1 - \Omega|^{-1/2} \quad (\text{A4})$$

otherwise. ε_{abc} is the Levi-Civita antisymmetric tensor, $\nabla = \partial/\partial\mathbf{q}$, \mathbf{S}^C is the cofactor matrix of \mathbf{S} and the function $\alpha(\tau) = 6/(\tau^2 + k)$ ($k = -1, 0$ or 1 for open, flat and closed models). The first equation (A2) is an evolution equation for \mathbf{S} , i.e. the equation of motion of a mass element, while the second equation (A3) is the irrotationality condition for the peculiar velocity \mathbf{v} in *Eulerian space*. The irrotationality condition restricts the set of solutions to the irrotational ones, which is reasonable in our cosmological context as any rotational mode is severely damped in the early linear evolution; see Buchert (1992) for a detailed discussion of this point. Another useful restriction on the solutions of equations (A2) and (A3) is the initial parallelism of peculiar velocity and acceleration, which is also supported by the growing modes in the linear and quasi-linear regime (Buchert 1992; Buchert & Ehlers 1993).

The perturbative expansion is performed as follows. We can write the displacement field \mathbf{S} as:

$$\mathbf{S}(\mathbf{q}, t) = \varepsilon\mathbf{S}^{(1)}(\mathbf{q}, t) + \varepsilon^2\mathbf{S}^{(2)}(\mathbf{q}, t) + \varepsilon^3\mathbf{S}^{(3)}(\mathbf{q}, t) + \mathcal{O}(\varepsilon^4), \quad (\text{A5})$$

where ε is a small parameter. Putting this expression into the evolution equations (A2, A3) for \mathbf{S} , and considering terms of order ε , ε^2 and ε^3 separately, one finds equations for the various $\mathbf{S}^{(n)}$ terms. It turns out that, at any order (as recently demonstrated by Ehlers & Buchert 1996), the solutions are separable in time and space. At first and second orders, the solutions are irrotational in Lagrangian space, i.e. the matrices $S_{a,b}^{(1)}$ and $S_{a,b}^{(2)}$ are symmetric. At the third order, the equation for $\mathbf{S}^{(3)}$ is not separable as it stands, but it is possible to divide the $\mathbf{S}^{(3)}$ term into three different modes, all separable in space and time:

$$\mathbf{S}^{(3)}(\mathbf{q}, t) = \mathbf{S}^{(3a)}(\mathbf{q}, t) + \mathbf{S}^{(3b)}(\mathbf{q}, t) + \mathbf{S}^{(3c)}(\mathbf{q}, t). \quad (\text{A6})$$

The third term, not reported by Bouchet et al. (1995) who consider only those terms which contribute to $S_{a,a}$, is a purely rotational mode in Lagrangian space ($S_{a,b}^{(3c)}$ is antisymmetric), and its existence is necessary to guarantee irrotationality in Eulerian space. This fact can be understood

in this way: the Lagrangian to Eulerian transformation is in general a non-Galileian one, so the rotational mode can be seen as an effect of inertial forces (see the discussions in Buchert 1994 and Catelan 1995).

Perturbative terms are listed in the following. The equations for the time functions b_n contain both growing and decaying modes, which have to be consistently considered in the calculations; however, for present purposes only the growing modes for each b_n are needed. The time functions are accurately described by the following expressions (exact for the first order):

$$\begin{aligned} b_1 &= -b(t) \\ b_2 &= -\frac{3}{14}b_1^2\Omega^{-a} \\ b_{3a} &= \frac{1}{9}b_1^3\Omega^{-b} \\ b_{3b} &= -\frac{5}{42}b_1^3\Omega^{-c} \\ b_{3c} &= \frac{1}{14}b_1^3\Omega^{-d}, \end{aligned} \quad (\text{A7})$$

where $b(t)$ is the linear growing mode. In an Einstein-de Sitter background it is simply:

$$b(t) = a(t). \quad (\text{A8})$$

In an open Universe, it is convenient to express the growing mode in terms of the time variable τ , equation (A4):

$$b(\tau) = \frac{5}{2} \left(1 + 3(\tau^2 - 1) \left(1 + \frac{\tau}{2} \ln \left(\frac{\tau - 1}{\tau + 1} \right) \right) \right). \quad (\text{A9})$$

The growing mode has been normalized so as to give $b(t) \simeq a(t)$ at early times. In a flat Universe with cosmological constant, it is useful to use $h = \coth(3H_0 t \sqrt{1 - \Omega_0/2})$ as time variable:

$$b(h) = h \int_h^\infty (x^2(x^2 - 1)^{1/3})^{-1} dx. \quad (\text{A10})$$

The coefficients a , b and c in equation (A7) have been calculated in Bouchet et al. (1992) and Bouchet et al. (1995), and are $a=2/63$, $b=4/77$ and $c=2/35$ in the non-flat cases, $a=1/143$, $b=4/275$ and $c=269/17875$ in the flat $\Lambda \neq 0$ cases. The above-cited authors have not estimated the Ω -dependence of the $3c$ term, as they do not take that term into account. However, as clarified in the text, the $3c$ term can be safely neglected. It can be appreciated that the b_2/b^2 and b_3/b^3 terms weakly depend on Ω when $\Omega \sim 1$; then, in a Universe with $\Omega_0 \geq 0.2$, as our Universe appears to be, the Ω dependence in equations (A7) can be safely neglected.

The spatial equations for the $\mathbf{S}^{(n)}(\mathbf{q})$ terms are Poisson equations. It is convenient to express $\mathbf{S}^{(1)}$, $\mathbf{S}^{(2)}$, $\mathbf{S}^{(3a)}$ and $\mathbf{S}^{(3b)}$ in terms of scalar potentials, and $\mathbf{S}^{(3c)}$ in terms of a vector potential:

$$\begin{aligned} \mathbf{S}^{(n)} &= \nabla\varphi^{(n)}, \quad n = 1, 2, 3a, 3b \\ \mathbf{S}^{(3c)} &= \nabla \times \boldsymbol{\varphi}^{(3c)}. \end{aligned} \quad (\text{A11})$$

Defining the principal and mixed invariants of one or two tensors as follows:

$$\mu_1(A_{ab}) = \text{tr}(A_{ab}) = A_{aa}$$

$$\begin{aligned}\mu_2(A_{ab}, B_{ab}) &= \frac{1}{2}(A_{aa}B_{bb} - A_{ab}B_{ab}) \\ \mu_2(A_{ab}) &= \mu_2(A_{ab}, A_{ab}) \\ \mu_3(A_{ab}) &= \det(A_{ab})\end{aligned}\quad (\text{A12})$$

(note that $\mu_1(\varphi_{,ab}) \equiv \nabla^2 \varphi$), it is possible to write the following equations for the potentials:

$$\begin{aligned}\varphi^{(1)} &= \varphi \\ \nabla^2 \varphi^{(2)} &= 2\mu_2(\varphi_{,ab}^{(1)}) \\ \nabla^2 \varphi^{(3a)} &= 3\mu_3(\varphi_{,ab}^{(1)}) \\ \nabla^2 \varphi^{(3b)} &= 2\mu_2(\varphi_{,ab}^{(1)}, \varphi_{,ab}^{(2)}) \\ \nabla^2 \varphi_a^{(3c)} &= \varepsilon_{abc} \varphi_{,cd}^{(1)} \varphi_{,db}^{(2)}.\end{aligned}\quad (\text{A13})$$

The first equality is a consequence of initial conditions. Cate-
lan (1995) gives expressions for the Fourier transforms of the
solutions of all these equations, which are useful for calcu-
lating, e.g., mean values of the perturbing terms.

APPENDIX B: ELLIPSOIDAL COLLAPSE

Let $\varphi(\mathbf{q})$ be a quadratic potential in its principal reference
frame:

$$\varphi(\mathbf{q}) = \frac{1}{2}(\lambda_1 q_1^2 + \lambda_2 q_2^2 + \lambda_3 q_3^2). \quad (\text{B1})$$

It is easy to calculate all the perturbative terms in this
case, especially if the local forms are used (see Buchert &
Ehlers 1993, Buchert 1994 and Catelan 1995 for further de-
tails):

$$\begin{aligned}\varphi_{,a}^{(2L)} &= \varphi_{,a} \varphi_{,bb} - \varphi_{,ab} \varphi_{,b} \\ \varphi_{,a}^{(3aL)} &= \varphi_{,ab}^C \varphi_{,b} \\ \varphi_{,a}^{(3bL)} &= 1/2(\varphi_{,a} \varphi_{,bb}^{(2)} - \varphi_{,b} \varphi_{,ab}^{(2)} + \varphi_{,a}^{(2)} \varphi_{,bb} - \varphi_{,b}^{(2)} \varphi_{,ab}) \\ \varphi_a^{(3cL)} &= 1/2(\varphi_{,b} \varphi_{,ab}^{(2)} - \varphi_{,b}^{(2)} \varphi_{,ab});\end{aligned}\quad (\text{B2})$$

$\varphi_{,ab}^C$ is the cofactor matrix of $\varphi_{,ab}$. These local parts are exact
solutions in our case, as they are irrotational; their expres-
sions can be considerably simplified, as all the derivatives
beyond the second vanish. The outcoming contributions to
the deformation tensor have been given in equation (11).
A technical remark on the 3b contribution: Buchert (1994)
divides this contribution into two parts, weighted by two co-
efficients whose sum is equal to one (see his equations 27).
These two coefficients could be varied in order to make the
whole contribution irrotational. On the other hand, Cate-
lan gives an expression analogous to the one given here (see
his equation 44); this would correspond to a choice of 1/2
for the two coefficients of Buchert. As a matter of fact, the
two parts identified by Buchert are irrotational by them-
selves in the ellipsoidal case, and have the same divergence,
but are nonetheless different. Using only one or another,
which would correspond to setting one coefficient to 1 and
the other to 0, makes the Lagrangian series no to converge
any more to the numerical solution. So, the choice of 1/2 for
both coefficients seems the right one for ellipsoidal collapse.

All the contributions to the deformation tensor are di-
agonal in the same frame; the 3c contribution obviously van-
ishes. The diagonal (1,1) components are:

$$\begin{aligned}\varphi_{,11} &= \lambda_1 \\ \varphi_{,11}^{(2)} &= \lambda_1(\lambda_2 + \lambda_3) \\ \varphi_{,11}^{(3a)} &= \lambda_1 \lambda_2 \lambda_3 \\ \varphi_{,11}^{(3b)} &= \lambda_1 \lambda_2 \lambda_3 + \lambda_1 \delta_l(\lambda_2 + \lambda_3)/2,\end{aligned}\quad (\text{B3})$$

where $\delta_l = \lambda_1 + \lambda_2 + \lambda_3$. The Jacobian determinant van-
ishes when one of its eigenvalues vanishes. Then, if the Ω
dependence of the time functions is neglected, it is possi-
ble to write the $J = 0$ equation as a third-order algebraic
equation:

$$1 - \lambda_i b_c - \frac{3}{14} \lambda_i (\delta_l - \lambda_i) b_c^2 - \left(\frac{\mu_3}{126} + \frac{5}{84} \lambda_i \delta_l (\delta_l - \lambda_i) \right) b_c^3 = 0, \quad (\text{B4})$$

where b is the linear growing mode, and $\mu_3 = \lambda_1 \lambda_2 \lambda_3$. Note
how higher-order coefficients become increasingly smaller.

In the spherical case, the equation reduces to:

$$1 - \frac{1}{3}(\delta_l b_c) - \frac{1}{21}(\delta_l b_c)^2 - \frac{23}{1701}(\delta_l b_c)^3 = 0, \quad (\text{B5})$$

which, if truncated at first, second, or third-order, gives the
solutions:

$$\begin{aligned}b_c^{(1)} &= 3/\delta_l \\ b_c^{(2)} &= 2.27/\delta_l \\ b_c^{(3)} &= 2.05/\delta_l.\end{aligned}\quad (\text{B6})$$

The complete equation at first-order gives the well
known Zel'dovich approximation:

$$b_c = 1/\lambda_i. \quad (\text{B7})$$

It is apparent that the 1-axis, corresponding to the largest λ
eigenvalue, is the first to collapse. The second-order solution
is:

$$b_c^{(2)} = \frac{7\lambda_1 - \sqrt{7\lambda_1(\lambda_1 + 6\delta_l)}}{3\lambda_1(\lambda_1 - \delta_l)}. \quad (\text{B8})$$

This solution is limited to $\delta_l \geq -\lambda_1/6$, i.e. to overdensities
or weak underdensities. The other solution of the equation
(with a plus in front of the square root) is either negative
or larger than the chosen one, except when $\delta_l < \lambda_i < 0$. In
this case, which includes spherical voids, the second solution
incorrectly predicts collapse. The bad behaviour of second-
order perturbations in predicting the dynamics of voids had
already been noted by Sahni & Shandarin (1995). Finally,
it is possible to verify, by differentiating equation (B8) with
respect to the λ_i parameter, that the 1-axis is the first to
collapse.

To obtain the third-order solution, let $y = \delta_l/\lambda_i$, and
 $D = \mu_3 \lambda_i^3/126 + 5y(y-1)/84$; then let

$$Q = (3(y-1)^2 - 196D)/588D^2$$

$$R = (2(y-1)^3 - 196(y-1)D - 2744D^2)/5488D^3$$

When $R^2 - Q^3 > 0$, which is valid for spherical and quasi
spherical perturbations, the solution is:

$$b_c = -\frac{\text{sgn}(R)}{\delta_l} \left(\left(\sqrt{R^2 - Q^3} + |R| \right)^{1/3} + Q \left(\sqrt{R^2 - Q^3} + |R| \right)^{-1/3} \right) - \frac{(y-1)}{14D}. \quad (\text{B9})$$

In this case, it is possible to show analytically that the 1-axis is the first to collapse. Otherwise, the solution has to be chosen as the smallest non-negative one between:

$$\begin{aligned} b_{c1} &= -2\sqrt{Q} \cos(\theta/3) - (y-1)/14D \\ b_{c2} &= -2\sqrt{Q} \cos((\theta + 2\pi)/3) - (y-1)/14D \\ b_{c3} &= -2\sqrt{Q} \cos((\theta + 4\pi)/3) - (y-1)/14D, \end{aligned} \quad (\text{B10})$$

where $\theta = \arccos(R/\sqrt{Q^3})$. It has been checked with the computer that the 1-axis is the first to collapse.

The evolution equations of the homogeneous ellipsoid, which have been numerically integrated, are analogous to the ones in M95: let $r_i(t) = a_i(t)q_i$ be the physical i -th coordinate of the outer surface of the ellipsoid, in the principal-axes system; q_i is the initial – Lagrangian – position and a_i is the expansion factor for the i -th axis. The universal scale factor is called a , without pedix. Then the evolution equations for the a_i factors are:

$$\begin{aligned} \frac{d^2 a_i}{da^2} - (2a(1 + (\Omega_0^{-1} - 1)a))^{-1} \frac{da_i}{da} \\ (2a^2(1 + (\Omega_0^{-1} - 1)a))^{-1} a_i \left[\frac{1}{3} + \frac{\delta}{3} + \frac{b'_i}{2} \delta + \lambda'_{vi} \right] \end{aligned} \quad (\text{B11})$$

in the open case and

$$\begin{aligned} \frac{d^2 a_i}{da^2} - \frac{1 - 2(\Omega_0^{-1} - 1)a^3}{2a(1 + (\Omega_0^{-1} - 1)a)} \frac{da_i}{da} + \\ (2a^2(1 + (\Omega_0^{-1} - 1)a))^{-1} a_i \left[\frac{1}{3} + \frac{\delta}{3} + \frac{b'_i}{2} \delta + \lambda'_{vi} \right] \end{aligned} \quad (\text{B12})$$

in the flat case with cosmological constant. Here (a_0 is the initial scale factor):

$$\delta = \frac{a^3}{a_1 a_2 a_3} - 1 \quad (\text{B13})$$

$$b'_i = \frac{2}{3} [a_i a_j a_k R_D(a_i^2, a_j^2, a_k^2) - 1] \quad i \neq j \neq k \quad (\text{B14})$$

$$\lambda'_{vi} = -\frac{a}{a_0} \left(\frac{\delta}{3} - a_0 \lambda_i \right) \quad (\text{B15})$$

$$R_D(x, y, z) = \frac{3}{2} \int_0^\infty \frac{d\tau}{(\tau + x)^{1/2} (\tau + y)^{1/2} (\tau + z)^{3/2}}. \quad (\text{B16})$$

This Carlson's elliptical integral has been calculated by means of the routine given by Press & Teukolsky (1990).

The initial conditions are:

$$a_i(a_0) = a_0(1 - a_0 \lambda_i) \quad (\text{B17})$$

$$\frac{da_i}{da}(a_0) = \frac{1}{a_0} (a_i(a_0) - a_0^2 \lambda_i). \quad (\text{B18})$$

This paper has been produced using the Royal Astronomical Society/Blackwell Science L^AT_EX style file.